Center-to-limb variation of the second solar spectrum

J.O. Stenflo[1], **M. Bianda**[2], **C.U. Keller**[3], **and S.K. Solanki**[1]

[1] Institute of Astronomy, ETH Zentrum, CH-8092 Zurich, Switzerland
[2] Istituto Ricerche Solari Locarno (IRSOL), Via Patocchi, CH-6605 Locarno-Monti, Switzerland
[3] National Solar Observatory, P.O. Box 26732, Tucson, AZ 85726-6732, USA

Abstract. The linear polarization that is caused by scattering processes in the solar atmosphere has been refered to as the "second solar spectrum", since it is structurally as rich as the ordinary intensity spectrum but quite different in appearance and information contents. One of the most used and theoretically best understood lines in the second solar spectrum is the Sr I 4607 Å line, which has served as a diagnostic tool for determinations of spatially unresolved, turbulent magnetic fields via the Hanle effect. Here we present the detailed center-to-limb variation of the scattering polarization in this line for a number of new data sets obtained both with an electrooptical modulation system (ZIMPOL) and a non-modulating beam splitter system (at IRSOL, Locarno), to provide improved observational constraints for theoretical modelling. The amplitude and width of the polarization profile, the amount of continuum polarization, as well as the depth and width of the intensity profile have been evaluated and carefully corrected for spectral broadening and stray light. While there is generally good agreement between the five data sets, some systematic differences are shown to be of solar rather than instrumental origin, most likely due to spatially varying Hanle depolarization across the solar disk.

A number of other spectral lines have been observed with the ZIMPOL system at two different limb distances ($\mu = 0.1$ and 0.2) to allow us to compare the steepness of the center-to-limb variation of their polarization amplitudes. The steepest variation is exhibited by the continuum polarization, which declines by approximately a factor of 6 when going the 15 arcsec distance from $\mu = 0.1$ to $\mu = 0.2$. The spectral lines with the steepest center-to-limb variation are molecular lines, the Ca II infrared triplet, and Hα. In contrast the Sr I 4607 and Ba II 4554 Å lines have only moderately steeper center-to-limb variations than that of an ideal, purely dipole-scattering atmosphere, for which the polarization ratio between $\mu = 0.1$ and $\mu = 0.2$ is 1.38. These center-to-limb variations may be used to constrain temperature-density models of the upper photosphere and chromosphere.

Key words: polarization – scattering – techniques: polarimetric – Sun: atmosphere; general; magnetic fields

Send offprint requests to: J.O. Stenflo

1. Introduction

Near the Sun's limb the solar spectrum becomes linearly polarized due to scattering processes, which are basically non-magnetic in origin but become modified by magnetic fields via the Hanle effect. The polarized spectrum is as rich in spectral structures as the ordinary intensity spectrum but differs in appearance and information contents (Stenflo & Keller 1996, 1997). It has therefore been found convenient to refer to it as the "second solar spectrum".

Although an increasing number of spectral regions have been surveyed near the limb, generally at a disk position defined by μ (the cosine of the heliocentric angle) =0.1 (which is about 5 arcsec inside the extreme limb), little observational data on the actual center-to-limb variations (CLV) of the scattering polarization have been available. The prime CLV data set previously published goes back to observations made in 1978 (Stenflo et al. 1980) for a few selected spectral lines.

In this old data set it is the CLV of the Sr I 4607 Å line that has received the most attention, since this line lends itself well to detailed modelling with numerical radiative transfer (Faurobert-Scholl 1993; Faurobert-Scholl et al. 1995). This modelling has been performed mainly for the purpose of diagnosing "hidden" turbulent magnetic fields, a possibility that was first explored by Stenflo (1982). Such fields that are tangled or turbulent on scales that are beyond the attainable spatial resolution are invisible in any magnetogram. In contrast, the Hanle effect offers the best prospect for empirically exploring them.

The previous observations from 1978 suffered from limited spectral resolution, which meant that the narrow polarization peak in the line was reduced in amplitude by about 50 % by spectral smearing. The precise amount of spectral broadening and stray light was not determined but only estimated. Also, the reproducibility of the CLV curve has never been checked.

In the radiative-transfer modelling of Faurobert-Scholl (1993) and Faurobert-Scholl et al. (1995) the spectral smearing was accounted for by applying a macroturbulent broadening that would lead to agreement between the widths of the computed and observed intensity profiles at the various disk positions. Then the comparison between the modelled and observed polarization amplitudes showed that the amplitudes computed for

zero magnetic fields were too large. A fit could only be achieved if Hanle depolarization due to a turbulent field with a strength in the range 10–30 G was introduced.

In the present paper we present new data sets on the CLV of the Sr I line, obtained from five different observing runs with different instruments and observing procedures. The extracted parameters (widths and amplitudes of the polarization and intensity profiles) have been carefully corrected for both spectral broadening and stray light. The CLVs of all these calibrated and corrected parameters provide a more complete set of observational constraints for radiative-transfer modelling. The comparison between the data sets illustrates not only the magnitude of the observational uncertainties and the degree of reproducibility, but it also reveals that a substantial part of the spread in the data is due to intrinsically solar causes.

A byproduct of the work on the Sr line is the determination of the polarization of the continuum near the Sr line and its center-to-limb variation (CLV). We have also measured the slope of the CLV for a number of other spectral lines. An overview of these determinations is presented, which illustrates how the CLV slope differs for different categories of lines and compares with theoretical expressions. As the shapes and slopes of the CLV curves are sensitive functions of the atmospheric structure, they may serve as new constraints on models of the temperature-density stratification of the Sun's atmosphere.

2. Observational material

The following new data sets are presented here: (1) Observations with ZIMPOL I (the first generation of the **Z**urich **Im**aging Stokes **Pol**arimeter) made in June 1994, November 1994, and April 1995. (2) Observations at IRSOL, Locarno, on 22 September, 19 October, and 31 October 1995. While the ZIMPOL observations have been carried out at the McMath-Pierce facility of the National Solar Observatory (Kitt Peak, Arizona) with an electrooptical modulation-demodulation system (Povel et al. 1991; Keller et al. 1992; Stenflo 1994; Povel 1995), the IRSOL observations have been made with a stationary beam splitter without modulation but with alternate settings of a half-wave plate to eliminate gain table effects (see below).

2.1. ZIMPOL observations

During an observing run with ZIMPOL in June 1994 the Sr I 4607 Å line was recorded with the spectrograph slit oriented perpendicular to the solar limb, which allowed us in a single exposure to obtain the center-to-limb variation (CLV) as a continuous function from the extreme limb ($\mu = 0$) to $\mu \approx 0.3$. For this more exploratory observation no separate recording at disk center was made, which by comparison with FTS spectra could have allowed a direct determination of the spectral broadening and stray light.

The observing run with ZIMPOL in November 1994 was used to make more careful recordings with the spectrograph slit oriented parallel to the solar limb at a number of discrete positions to cover the full μ range from 0.1 to 1.0 that would
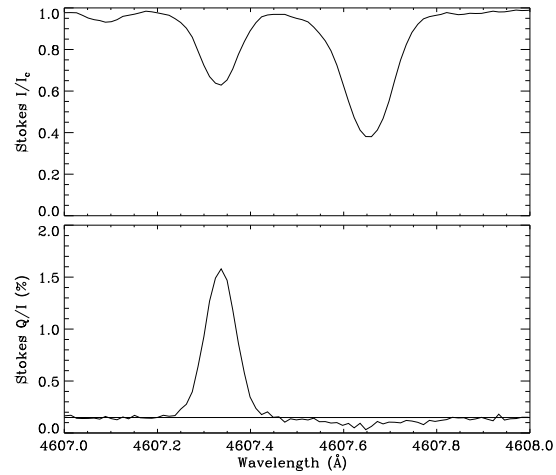

Fig. 1. Section of a recording at the position $\mu = 0.1$ of the solar disk with the ZIMPOL I polarimeter system attached to the main spectrograph of the McMath-Pierce facility at NSO/Kitt Peak. While the Sr I 4607.34 Å line to the left shows a symmetric and strong polarization peak, the Fe I 4607.65 Å line to the right depolarizes the continuum.

give us the complete CLV curve. As the different parts of the 49 arcsec long recorded section of the slit had the same value of μ, we could use spatial averaging along the slit to enhance the signal-to-noise ratio.

Fig. 1 shows an example of a 1 Å wide section of a recording at $\mu = 0.1$ that covered the Sr I line and its surroundings. Since the Sr polarization signal at this limb position is so strong, we used a short integration time resulting in an rms noise of about 7×10^{-5} in the degree of polarization. For most other ZIMPOL recordings in other spectral or spatial regions with weaker signals, we used longer integrations (usually about 10 min), corresponding to rms noise values of typically 2×10^{-5}.

While most other parts of the spectrum that we have explored with ZIMPOL have been recorded at the single limb distance of $\mu = 0.1$, we also observed a number of lines at $\mu = 0.2$. These observations were carried out during the observing runs of both November 1994 and April 1995.

The McMath-Pierce solar telescope suffers from substantial instrumental polarization, which is dealt with as described in Stenflo et al. (1983a) and Stenflo & Keller (1997) and will be commented on more in Sects. 3.3 and 3.4. The dominating term is Stokes $I \rightarrow Q$ cross talk, which is crudely compensated for with a tilting glass plate. The residual part of this cross talk leads to a spectrally flat offset of the zero level of the fractional polarization Q/I. The procedure to recover the lost zero point is described in Sect. 3.4.

2.2. IRSOL observations

The Gregory-Coudé system at IRSOL (Istituto Ricerche Solari Locarno) in Switzerland, with its 45 cm aperture vacuum telescope and Coudé-Echelle spectrograph, is identical to the corresponding German system (GCT) on Tenerife. It has the advantage of being a nearly polarization-free telescope around

the time of the equinox (21 March and 23 September), except for the polarization effects due to stresses in the vacuum windows. The instrumental polarization does not vary during the day but only with the Sun's declination. To optimize the observing conditions the observations were therefore carried out within 6 weeks of the fall equinox, on 22 September, 19 October, and 31 October.

The polarimetric system used consists of a polarizing beam splitter in front of the entrance slit, preceded by a half-wave plate with two different orientations, one neutral with the fast axis parallel to one of the polarizing directions, and one rotated by 45° such that the Stokes coordinate system gets rotated by 90°. To produce a polarization (Q/I) image two exposures with the CCD in the spectral focus are made, corresponding to the two settings of the half wave plate. Each exposure produces a pair of orthogonally polarized images that have identical seeing distortions. While the sign of the polarization signal is reversed between the two exposures, the sign of the spurious instrumental effects remains unchanged. By forming certain ratios between the set of four images, as described in Donati et al. (1990), Semel et al. (1993), and Keller (1996), it is possible to form an image of the fractional linear polarization Q/I that is almost free from both gain table and seeing noise, which are the two main noise sources. This technique turns out to work remarkably well and will be described in detail in a forthcoming article (Bianda et al., in preparation).

Although the major noise sources can be removed in this way, a fixed-pattern Q/I background remains, which we eliminate by making recordings at disk center, where the intrinsic scattering polarization is zero for symmetry reasons, but the fixed, spurious pattern remains the same. We thus alternate recordings at each μ position with recordings at disk center.

Even after removal of this fixed pattern there remains a small but spectrally flat instrumental offset, which makes the zero point of the polarization scale undetermined. This problem is dealt with in the same way as for the ZIMPOL observations (cf. Sect. 3.4). The standard deviation in the Q/I amplitudes, as determined from the rms noise in the Q/I continuum, is typically 0.05 % for the IRSOL data, while it is close to 0.01 % for the ZIMPOL data in the case of the Sr I measurements.

3. Reduction procedure

The recorded spectra need to be corrected for spectrograph stray light, which significantly affects the polarization amplitudes, spectral broadening, which affects both amplitudes and line widths, and Stokes $I \rightarrow Q$ instrumental cross talk, which displaces the Q/I zero level. The effect of stray light and spectral smearing can be modelled and determined by comparing Stokes I profiles recorded at disk center with corresponding FTS spectra. The true zero point of the polarization scale can be located and determined together with the continuum polarization, as described in Sect. 3.4.

3.1. Effect of stray light

Spectrograph stray light is produced after the polarization analysis has been optically completed. It therefore adds a contribution to the Stokes I signal but not to Stokes Q. The fractional polarization Q/I is affected because the intrinsic Stokes I is increased to the observed I_{obs}. The dominant portion of the stray light can be considered to be in the form of a spectrally flat background, which can be expressed as a fraction s of the intensity I_c of the continuous spectrum. Thus

$$I_{\mathrm{obs}} = I + sI_c . \tag{1}$$

If we can properly locate the level $I_{\mathrm{obs}, c}$ of the observed continuous spectrum we can use Eq. (1) to express the true relative intensity I/I_c in terms of its apparent, observed value, and the stray light fraction s.

3.2. Determination of stray light and spectral broadening

We have in the past made an FTS atlas of the quiet Sun at disk center (in 1978, in search for a turbulent magnetic field through the possible correlation between line width and Landé factor). FTS spectra can be considered free from any stray light and spectral broadening. We have modeled our observed Stokes I spectra at disk center by adding to the corresponding FTS spectrum stray light according to Eq. (1) and applying Gaussian smearing, until a good fit is obtained. Usually this is done with an iterative least squares fitting algorithm.

For our Sr I observations the values obtained for the stray light s and total half width b of the instrumental Gaussian profile through these fits are 10.5 % and 33 mÅ for the ZIMPOL observations of November 1994, 1.5 % and 33 mÅ for the IRSOL 1995 observations. In contrast to the McMath main spectrograph, where the overlapping, unwanted grating orders of the single-pass system are blocked by interference filters, the IRSOL spectrograph uses a predisperser which greatly reduces the stray light.

In the case of the ZIMPOL observations of June 1994 no disk center observations were made that could be used for a model fit, and the set-up had more of an exploratory test character, such that somewhat larger values of s and b are to be expected. Best consistency between the results from June 1994 with the other data sets is obtained if we for this set choose $s = 15$ % and $b = 50$ mÅ (see below).

For comparison we note that the spectral broadening of the previous observations of 1978 was estimated to be about 90 mÅ (Stenflo et al. 1980).

3.3. Instrumental polarization

Close to the solar limb at the position angle of geographical north or south (which is not far from the heliographic north or south poles), where all our observations have been made, Stokes V and U are usually intrinsically small, so that $V \rightarrow Q$ and $U \rightarrow Q$ cross talk is a minor problem. Sometimes significant Stokes V signals due to magnetic fields can infiltrate the Stokes

Q spectrum through instrumental polarization, but these spurious signals can always be recognized due to their characteristic anti-symmetric profiles and spatial structuring. Cross talk *from* Q to the other Stokes parameters can in principle reduce the Q amplitudes and thus affect the polarization scale, but model calculations of the McMath-Pierce solar telescope (Bernasconi, private communication) show that this may affect the scale by at most 0.5 % when observing near the solar limb at the geographic north or south directions (which we did), which is a negligible effect in comparison with the scale changes due to uncertainties in the μ position (limb distance). For observations at other position angles, which we have avoided, these effects can be substantially larger.

The main instrumental-polarization effect of concern for the present type of observations is thus cross talk $I \rightarrow Q$, which means that a fraction k of the intensity, including the stray light, is added to the intrinsic Q to form the apparent Q_{obs}:

$$Q_{\mathrm{obs}} = Q + kI_{\mathrm{obs}} . \tag{2}$$

When combining Eq. (2) with Eq. (1) to derive the true fractional polarization $p = Q/I$ from the apparent p_{obs}, we find that the effect of the $I \rightarrow Q$ cross talk is an almost spectrally flat zero-line offset or background, which deviates slightly from flatness due to the stray light, although this is a second-order effect. More details on such second-order effects can be found in Keller (1996).

Since the IRSOL observations were made near an equinox, the above effects are small from the outset. In the case of the ZIMPOL observations at NSO/Kitt Peak we minimized the effects by always setting a tilting glass plate in front of the modulator before each exposure such as to null out the average apparent polarization signal. For these reasons second-order effects can be disregarded.

3.4. Determination of the polarization zero level

Since the continuum is polarized by scattering processes, we cannot find any spectral region near the solar limb that with certainty has zero intrinsic polarization. At disk center on the other hand the spatially averaged continuum polarization is zero for symmetry reasons, which may lead us to believe that disk-center observations could be used to calibrate the true zero level. However, the difference in angle of incidence of about $\frac{1}{4}^{\circ}$ between disk center and limb at the McMath heliostat mirror gives rise to a differential instrumental polarization between disk center and limb on the order of 10^{-4}, and the absolute value of the $I \rightarrow Q$ cross talk varies by 10^{-4} in a matter of minutes. Therefore we have not been successful in trying to calibrate directly the absolute zero point of the polarization scale with sufficient accuracy ($< 10^{-4}$) by reference to disk center observations. Instead we have applied another, more indirect technique that we will now describe.

Stenflo et al. (1983a,b) found through statistical analysis of large portions of the second solar spectrum, using scatter plots of p_{obs} vs. I_{obs}, that in spectral regions without many intrinsically polarizing lines (but with at least one depolarizing line)

it was possible to identify a linear regression relation between polarization and intensity. Such a regression line can be extrapolated to $I_{\mathrm{obs}} = I = 0$, where Q/I must be intrinsically zero because the ratio between the polarizing continuum opacity and the depolarizing line opacity vanishes. The value reached by the regression line for $I = I_c$ must then represent the true continuum polarization p_c. The apparent linearity of the regression implies that the shape of spectral lines that have no intrinsic polarization but only depolarize the continuum must (statistically) be the same in terms of Q/I as in Stokes I. Such a linear relation may be theoretically expected for weak depolarizing lines, but empirically it seems to work as a statistical average for strong lines as well. This identity in profile shape can be expressed in the form

$$\frac{p_c - p}{p_c} = \frac{I_c - I}{I_c} . \tag{3}$$

The Fe I line immediately to the red side of the Sr I 4607 Å line (cf. Fig. 1) shows no sign of any intrinsic polarization but only depresses the continuum polarization. Assuming this depression to be of the form given by Eq. (3) we can determine both the amount of continuum polarization and the absolute zero point of the polarization scale. The resulting level of the continuum polarization is drawn as the horizontal line in Fig. 1.

The value of p_c that we determine this way near the Sr I line is for $\mu = 0.1$ approximately 1.6 times larger than the value that is theoretically predicted by the radiative-transfer code of Auer et al. (1980). If the Fe I line would not only be depolarizing but actually have some intrinsic polarization, then it would be shallower than the corresponding Stokes I profile, and our regression analysis based on Eq. (3) would produce too small a value for p_c. In this case our present determination would be an underestimate of p_c, and the discrepancy with the theoretical value would become even larger.

In most other spectral regions that we have explored with ZIMPOL the large majority of spectral lines have some intrinsic line polarization, and it is difficult to identify any purely depolarizing lines with any confidence. For these spectral regions we have used the following procedure to determine the zero point of the polarization scale: We assume that the *shape* of the wavelength variation of the continuum polarization p_c is correctly predicted by the theory of Auer et al. (1980), but we apply a global scaling with a factor of 1.62 to lock the theoretical curve to the empirical value determined by regression analysis for the Sr I region. Equipped with this scaled p_c level we shift the observed polarized spectrum such that the average polarization values for the points with the largest Stokes I values (that are closest to the continuum level) agree with our value for p_c. The shifted spectrum should then have the correct zero point of its polarization scale.

We recognize that this procedure is based on several shaky assumptions and therefore is subject to considerable uncertainty, but it appears to be the best that we can do at present, and it gives results that are consistent with previous measurements of the continuum polarization (see Sect. 4.2 below). We will consider these uncertainties more in Sect. 4.3.

3.5. Correction for spectral broadening

It is not possible to perform a general deconvolution of the observed spectra without knowledge of the precise shape of the instrumental profile, but for the purpose of calculating corrections to the values of the widths and amplitudes of the observed line profiles it is here sufficient to assume that both the line profiles and instrumental profile have Gaussian shapes. When convolving two Gaussians with each other their widths add quadratically to form a new Gaussian profile with unchanged area. If the amplitude (or line depth) and half width of the (Gaussian) line profile are observed to be a_{obs} and h_{obs}, respectively, while the smearing function has half width b, deconvolution gives

$$h = \sqrt{h_{\mathrm{obs}}^2 - b^2} \tag{4}$$

for the corrected half width, while the corrected amplitude is

$$a = a_{\mathrm{obs}} \, b_{\mathrm{obs}} / b \,. \tag{5}$$

For Stokes I the profile that we are correcting is the relative line depth $(I_c - I)/I_c$, while for $p = Q/I$ it is $p - p_c$, the polarization with respect to the continuum level. The half level of the polarization profile is the level halfway between p_c and p_{max}. After the amplitude of $p_{\mathrm{obs}} - p_c$ has been corrected, we have to add p_c again to obtain the corrected polarization amplitude with respect to the zero point of the polarization scale.

No Fourier smoothing has been applied to the ZIMPOL data, but due to the larger polarization noise level of the IRSOL data it was needed to smooth the Q/I spectra before amplitudes and line widths were determined. As Fourier smoothing leads to some non-Gaussian spectral broadening, we have determined by numerical simulation the half width of a Gaussian smearing function that produces the same broadening as the Fourier filter that was applied. This half width depends on the width of the profile to be smeared due to the non-Gaussian nature of the Fourier filter function. For the range of widths occuring in our data the additional smearing due to the Fourier filter corresponds to half widths of 18–28 mÅ for an equivalent Gaussian smearing function. These widths add quadratically to the instrumental smearing of 33 mÅ, which leads to an effective broadening of the Q/I profiles that is larger but well defined.

4. Results

4.1. Comparison between the different data sets

Fig. 2 provides an overview of the center-to-limb variation (CLV) of the Sr I 4607 Å line for all the data sets together. The ZIMPOL data from June 1994 are represented by plusses, those from November 1994 by asterisks, while the IRSOL 1995 data are plotted as diamonds (for 22 September), triangles (for 19 October), and squares (for 31 October). The two upper panels refer to the fractional linear polarization Q/I, the lower panels to Stokes I.

All data sets have been corrected for spectral smearing and stray light as well as instrumental $I \to Q$ cross talk as described

in Sect. 3. The values given here therefore represent our best estimates of the intrinsic, solar values. Before these corrections were applied the results from the different data sets differed greatly, but Fig. 2 shows that after correction there is general agreement and consistency between the data sets. Some systematic differences remain, however, which we will comment on later. The spread of the data points gives us a feeling for the degree of reproducibility of the results. Although much of this spread may be of instrumental origin, there is clear evidence that part of the variation is intrinsically solar.

This evidence is directly seen in the top left panel, where we have plotted both the Q/I amplitude in the line (upper set of points) and the continuum polarization p_c (lower set of points). The Q/I amplitude is measured from the true zero point of the polarization scale, which has been determined together with p_c from the neighboring Fe I line as described in Sect. 3.4. As the June 1994 observations were made with the slit perpendicular to the limb, we obtain a smooth CLV curve from a single exposure with the CCD. The CLV of the Q/I amplitude shows a very pronounced kink near $\mu = 0.2$. Closer to the limb the amplitudes from November 1994 are considerably larger than those from June 1994, but the agreement is good for $\mu > 0.2$.

We see no possibility that such a kink in the curve obtained from a single exposure could be produced by instrumental effects, so we conclude that it must be intrinsically solar. $\mu = 0.2$ corresponds to a limb distance of about 20 arcsec. The most natural explanation for the kink is that for the June 1994 observations the slit happened to cut across a region that had more of Hanle-depolarizing magnetic fields inside the 20 arcsec limb zone as compared with the case for the November 1994 observations.

With other (not yet published) ZIMPOL observations in other spectral lines we have found unexpectedly large spatial variations of the Hanle depolarization effect. The best evidence that these variations are really due to the Hanle effect comes from observing the *differential* changes (line ratios) of the polarization amplitudes for combinations of lines with different Hanle sensitivities.

The magnitude of the continuum polarization is less than 10 % of the polarization amplitude in the Sr line. p_c has a much steeper center-to-limb variation as compared with the line polarization, as we will see more clearly later. It becomes approximately zero already at $\mu = 0.3$.

The Stokes I profile becomes shallower by a factor of two when going from disk center, where the line depth is about 0.6, to the limb, where it is about 0.3.

The line width increases from disk center towards the limb, both for Q/I and I. The Q/I width is smaller than the Stokes I width by about 30 %, which is typical when comparing the second solar spectrum with the intensity spectrum. Much of the Stokes I broadening is due to saturation involving optically thick radiative transfer, while the polarization profiles are not subject to this type of saturation. This is well illustrated by the Ba II 4554 Å line (Stenflo & Keller 1996, 1997), for which the polarization profile exhibits spectrally resolved hyperfine structure splitting, while this splitting is invisible in the corre-
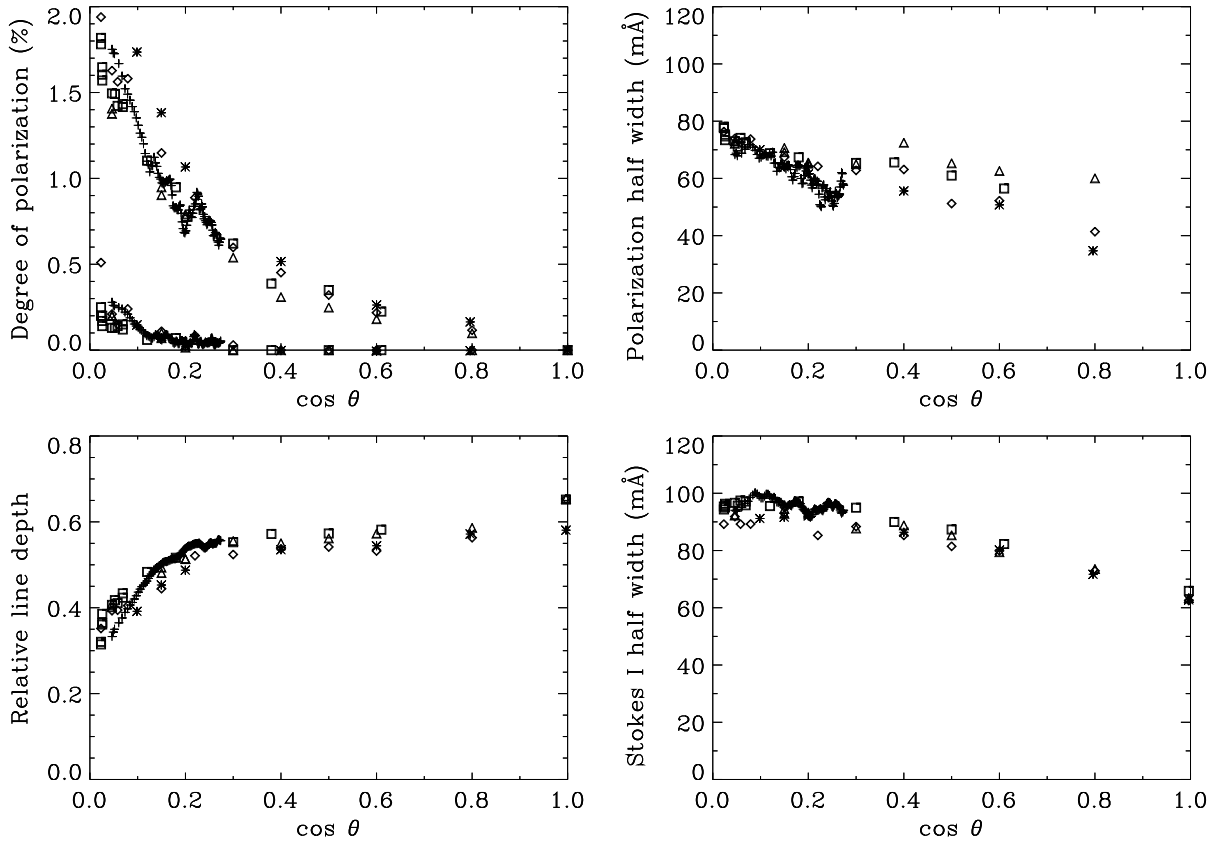
Fig. 2. Overview of the center-to-limb variation of the Sr I 4607 Å line parameters. θ is the heliocentric angle ($\mu = \cos\theta$). Top left panel: Polarization (Q/I) amplitude of the Sr I line (upper set of points) and continuum polarization p_c (lower set of points). Top right panel: Total half width of the polarization peak ($p - p_c$) of the Sr line. Lower left panel: Relative line depth of the Sr Stokes I profile. Lower right panel: Total half width of the Sr Stokes I profile. Pluses and asterisks represent ZIMPOL data from June and November 1994, respectively, while diamonds, triangles, and squares represent IRSOL data from 22 September, 19 October, and 31 October 1995, respectively.

sponding Stokes I profile, since it is masked by saturation line broadening.

We do not know why the June 1994 data show such a steep CLV for the width of the polarization peak, in particular in comparison with the IRSOL data.

4.2. Shapes of the polarized CLVs

The data set of the ZIMPOL November 1994 observing run has by far the smallest noise and the most detailed calibration. We therefore select it to compare in Fig. 3 the shape of the center-to-limb variation of the Sr I amplitude with that of the continuum polarization as well as with the theoretical curve (Chandrasekhar 1950) for an ideal, purely scattering atmosphere.

To facilitate a direct comparison of the shapes of the various curves we have multiplied the continuum polarization by a factor of 12 such that it approximately equals the Sr polarization at $\mu = 0.1$, while the theoretical Chandrasekhar curve has been scaled by the factor 0.2. We see that the CLV of the continuum polarization is by far the steepest, while a purely scattering atmosphere has the smallest slope.

We have found that the following analytical expression provides a good fit to the observed values for the polarization maximum of the line:

$$p_{\max} = \frac{a(1 - \mu^2)}{(\mu + b)} . \tag{6}$$

The theoretical considerations leading to the choice of this particular functional form will be discussed at the end of Sect. 4. We have chosen the parameter values $a = 0.3\%$ and $b = 0.07$ to fit our Sr I data and plotted the resulting function as the dashed curve in Fig. 3. For the continuum polarization we have made a parabolic fit with p_c given by

$$p_c(\%) = 0.37 - 2.73\mu + 4.97\mu^2 \tag{7}$$

as long as this function is positive, otherwise p_c is set =0. We plot 12 times this function as the dotted curve in Fig. 3.

The slightly negative values of the continuum polarization for $\mu \geq 0.4$ are not significant. For these μ values no depolarization of the neighboring Fe I line can be seen, and the almost horizontal regression line in the Q/I vs. I fit may formally have a slope that corresponds to a small negative polarization, but zero polarization is consistent with the error bars.
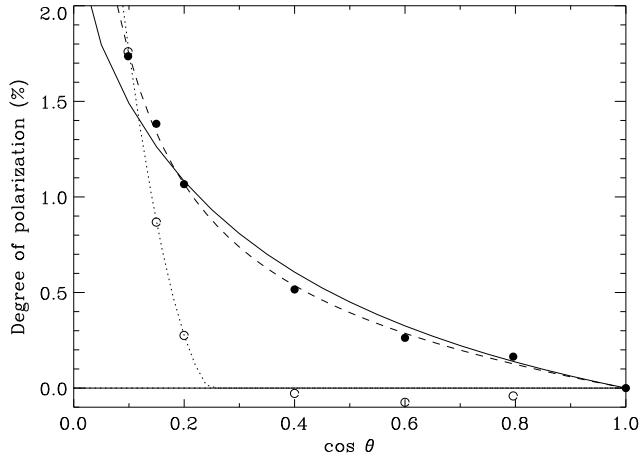
Fig. 3. Comparison between the shapes of three center-to-limb variation curves. The filled circles represent the values of the polarization maximum in the core of the Sr I 4607 Å line, observed with ZIMPOL in November 1994, and fitted with an analytical function (dashed curve) given by Eq. (6) for the parameter values $a = 0.3\%$ and $b = 0.07$. The open circles represent $12p_c$, where p_c is the continuum polarization determined from the same November 1994 data set. The dotted curve is a parabolic fit given by Eq. (7). The solid curve represents Chandrasekhar's (1950) solution for an ideal, purely scattering atmosphere, multiplied by a factor of 0.2.

It is interesting to note that both the magnitude and steepness of the continuum polarization in Fig. 3 are fully consistent with previous direct broad-band measurements in continuum windows of the solar spectrum (Mickey & Orrall 1974; Wiehr 1975; Leroy 1977). This supports the validity of our method to determine the zero point of the polarization scale.

In Fig. 3 the Sr polarization at $\mu = 0.8$ is anomalously high, considerably higher than the corresponding values of all the other data sets (cf. Fig. 2). It should therefore not be considered representative for the typical CLV. At $\mu = 0.8$, which is as much as 6.4 arcmin from the limb, the November 1994 recording showed spatially varying Stokes V-like anti-symmetric polarization profiles along the slit due to instrumental $V \rightarrow Q$ cross talk in combination with longitudinal magnetic fields. The spatial locations of these cross-talk effects were identified by their longitudinal Zeeman-effect signatures in the neighboring Fe I line and excluded from the evaluation of the Q/I profile of the Sr line. As however this μ position was not clean with respect to Zeeman-effect signatures in comparison with the other regions analysed, we have reasons to have less confidence in this data point.

The amount of scattering polarization that we observe at a given disk location depends in the case of a spherically symmetric sun primarily on the degree of limb darkening (anisotropy of the radiation field) seen by the last scattering particle, on the fraction of the opacity that is due to scattering, and on the intrinsic polarizability of each scattering process (i.e., the fraction of scattering processes that behave like classical dipole-type scattering). For line transitions we also have to consider the frac-

tion of scattering processes that are undisturbed by depolarizing collisions (which depends on the ratio between the spontaneous emission rate and the collision rate), as well as Hanle depolarization effects due to external magnetic fields.

The continuum is polarized by Rayleigh scattering by neutral hydrogen and Thomson scattering by free electrons. Both processes behave like classical dipole scattering, which represents the maximum attainable intrinsic polarizability, and this is also the case for scattering in the Sr line. Below the temperature minimum the continuum opacity is dominated by H^-, which is non-polarizing. Around the temperature minimum, where the degree of ionization is the smallest, the relative contribution from Rayleigh scattering by neutral hydrogen reaches a maximum (near 20 %), while higher up Thomson scattering by free electrons dominates the continuum opacity. Since the continuum is generally formed deep in the atmosphere, while the scattering part of the continuum opacity becomes significant only rather high up, continuum polarization only shows up near the extreme limb, for $\mu < 0.3$, and is expected to increase very steeply, as observed. The quantitative values are sensitive to the temperature-density structure of the atmosphere.

For a spectral line like the Sr I line the line-to-continuum opacity ratio increases with height, and the rate of depolarizing collisions rapidly declines due to the exponential density drop. Therefore the fraction of line scattering processes that are undisturbed by collisions approaches unity with height. For these reasons we expect the CLV of the line polarization to be steeper than that of an ideal, purely scattering atmosphere.

4.3. CLV behavior of different spectral lines

We have made recordings with ZIMPOL in November 1994 and April 1995 not only at $\mu = 0.1$ but also at $\mu = 0.2$ for a number of lines. It is of interest to compare the steepness of the center-to-limb variation in the different lines by deriving the ratio between the line polarizations measured at $\mu = 0.2$ and 0.1, and to compare it with the corresponding ratio for the continuum polarization and the Chandrasekhar curve for a purely scattering atmosphere.

In many or even most spectral regions the magnitude of the continuum polarization is comparable to that of the line polarization. Thus, if we would measure the line polarization from the polarization zero level, the results would to variable degrees be affected by the behavior of the continuum rather than of the lines alone. In addition, the amount of continuum polarization cannot be determined well in regions with no well-defined depolarizing lines, and unfortunately most spectral regions are like that.

Although the amount of continuum polarization p_c is difficult to determine, it is much easier to locate the relative level of the continuum by averaging Q/I for the highest I values (which are closest to the continuum level). Thus $p - p_c$ is a well-defined observational quantity that does not depend on the zero-point of the polarization scale and is a first approximation of the polarization that is due to the lines alone.
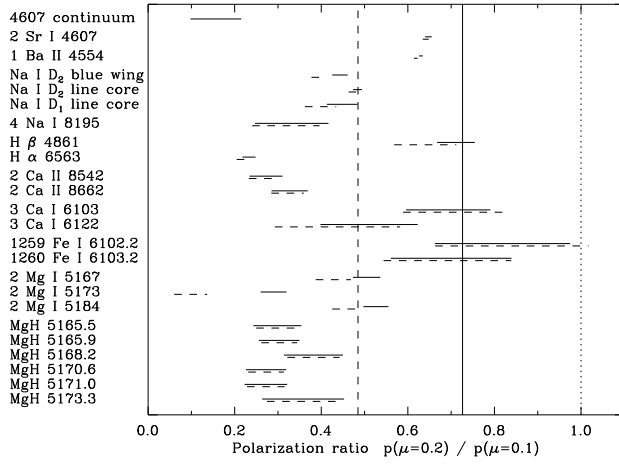
Fig. 4. Overview of the slopes of the center-to-limb variations for a number of lines observed with ZIMPOL in November 1994 and April 1995. The slopes are represented by the ratio between the Q/I polarizations observed at $\mu = 0.2$ and $\mu = 0.1$. The horizontal lines represent error bars. For the various spectral lines the solid error bars represent the p_{line} ratio, where p_{line} is defined by Eq. (8), while the dashed error bars represent the $p - p_c$ ratio. For the 4607 Å continuum it is simply the p_c ratio that is given. The Chandrasekhar (1950) ratio of 0.726 for a purely scattering atmosphere is given by the solid vertical line, while the corresponding ratio of 0.485 for the analytical function $(1 - \mu^2)/\mu$ is given by the vertical dashed line. For an optically thin scattering layer the CLV function should be proportional to $(1 - \mu^2)/[\mu I_c(\mu)]$, which at 5000 Å gives a polarization ratio of 0.37.

$p - p_c$ however does not represent the entire line polarization, since in the complete absence of intrinsic line polarization the amount of polarization at line center would not be p_c, but there would be a depression below the continuum level. The contribution p_{line} from the spectral line to the total polarization p (line plus continuum) should rather be measured from this depressed level. This was done in Stenflo et al. (1983a) by defining p_{line} as

$$p_{\text{line}} = p - p_c + p_c d, \qquad (8)$$

where d is the Stokes I line depth. We see from Eq. (8) that we in the absence of intrinsic line polarization ($p_{\text{line}} = 0$) retrieve Eq. (3) for purely depolarizing lines, as expected. p_{line} thus represents the additional polarization that is contributed by the line.

Fig. 4 provides an overview of the results for the various lines that we have observed. The horizontal lines represent error bars based on an assumed error of 0.003 % in p and p_c (0.006 % is used for Sr I and its neighboring continuum, since shorter exposures were used due to the larger Sr signals). This error is in most cases larger than the actual formal noise and is therefore conservatively chosen. The solid error bars represent for the spectral lines the ratio of the p_{line} values derived from Eq. (8) at $\mu = 0.2$ and 0.1, respectively, while the dashed lines represent for comparison purposes the corresponding ratios of the $p - p_c$ values. In the case of the 4607 Å continuum the solid line simply represents the p_c ratio. For reference purposes we have also

marked by the solid vertical line the Chandrasekhar (1950) value of 0.726 for a purely scattering atmosphere.

The data of Fig. 4 have been corrected for stray light but not for finite spectral resolution. The correction factors for spectral broadening should however be approximately the same for $\mu = 0.1$ and 0.2, so to first order these factors divide out when forming the ratios that represent the CLV slopes.

The error bars of the determined polarization ratio become large when the polarization amplitudes are small, approximately in inverse proportion to the amplitudes, and we divide by small numbers. In several cases, when the continuum polarization is not small in comparison with the line polarization, the positions of the solid and dashed error bars disagree significantly. It is the solid lines representing the p_{line} ratio that are the more relevant ones for the line polarization, and they show a somewhat more consistent behavior than the dashed lines.

Fig. 4 shows that the CLV of the continuum polarization is steeper than that of any line polarization that we have examined. The steepest p_{line} variations are exhibited by the molecular MgH lines, the Ca II infrared lines (8542 and 8662 Å), Hα, and Na I 8195 Å. For these lines the polarization declines by about a factor of 3 when going from $\mu = 0.1$ to $\mu = 0.2$, as compared with a factor of 6 for the continuum polarization and 1.38 for a purely scattering atmosphere. The CLVs of Sr I and Ba II are only slightly steeper than the CLV of the purely scattering atmosphere, while the Fe I lines that we have looked at agree with the purely scattering case at least within the fairly large error bars.

The molecular lines are expected to be formed in a thin layer in the lower portion of the temperature minimum region, since the optimum conditions for molecule formation requires a combination of low temperature and high density. This layer is well above the layers from where most of the photons at these wavelengths emanate (optical depth unity). For a plane-parallel stratification the optical path length of the optically thin molecular layer scales with μ as $1/\mu$. The source function for Stokes Q on the other hand scales as $1 - \mu^2$ (Stenflo 1994). Therefore it is natural to expect the shape of the resulting CLV to be proportional to the function $(1 - \mu^2)/\mu$, which explains the logic behind the choice of function in Eq. (6), where we in addition entered a parameter b in the denominator to control the slope of the analytical function. As the plane-parallel approximation breaks down when approaching the extreme limb, there will be some saturation of the $1/\mu$ part of the CLV curve at the extreme limb.

As pointed out to us by M. Faurobert-Scholl (private communication) we also need to multiply the function $(1 - \mu^2)/\mu$ with $1/I_c(\mu)$ to make it a more complete representation of the CLV for weak lines formed by scattering in an optically thin layer, like our molecular lines. The reason is that while Stokes Q as the nominator in the fractional polarization Q/I scales with $(1 - \mu^2)/\mu$, the intensity I is approximately given by the continuum intensity at that μ position, $I_c(\mu)$. While the $\mu = 0.2/\mu = 0.1$ ratio for the function $(1 - \mu^2)/\mu$ is 0.485, the corresponding ratio for $I_c(\mu)$ is wavelength dependent. Since the ratio for the function $(1 - \mu^2)/[\mu I_c(\mu)]$ would therefore not

be a straight line in Fig. 4, we have only plotted the 0.485 value as the vertical dashed line in the figure for reference purposes. At 5000 Å the observed value of $I_c(0.1)/I_c(0.2)$ is 0.76 (Allen 1973). The molecular MgH lines should therefore be compared with the ratio $0.76 \times 0.485 = 0.37$ for an optically thin scattering layer. This value comes close to the observed polarization ratios in Fig. 4.

While these considerations provide a good explanation for the steep CLV of optically thin lines like the molecular lines, they are not applicable to our optically thick lines, whose CLV will be governed by more complex radiative-transfer effects. We note in particular that lines like the Sr line has a less steep CLV than the function $(1 - \mu^2)/\mu$, while a number of other optically thicker lines, like Hα and the Ca II infrared triplet, have a steeper variation.

5. Concluding remarks

We have assembled the available new observational data on the center-to-limb variation (CLV) of the scattering polarization for various spectral lines and the continuum, and have presented the results in a form that may be directly used to constrain theoretical models. Although some information on the slope of the CLV curve is available for a number of different spectral lines, the only line for which the full CLV curve has been investigated in detail (apart from a few CLV curves from 1978 observations (Stenflo et al. 1980)) is the Sr I 4607 Å line. The main reasons for the attention that this line has received are: (1) It has an unusually strong and symmetric polarization peak that is surrounded by a clean continuum and an adjacent depolarizing Fe I line that can be used for reference purposes and for the determination of the continuum level and the zero point of the polarization scale. (2) Its $J = 0 \rightarrow 1 \rightarrow 0$ resonant scattering transition is the quantum mechanical analog to classical dipole scattering, which represents the maximum polarizing case. (3) Its atomic structure and radiative-transfer parameters are well known. (4) It lends itself well to modelling with radiative transfer, in particular since it is sufficient to assume complete frequency redistribution rather than having to do the full partial redistribution problem, because it is not strong enough to have extensive wings, so all the significant polarization occurs in the Doppler core. (5) Due to these possibilities for detailed quantitative modelling, it has been extensively used to diagnose the strength of the "hidden", spatially unresolved turbulent magnetic field of the Sun (Faurobert-Scholl 1993; Faurobert-Scholl et al. 1995).

The present observations give the detailed CLV of the Sr I line not only for the polarization amplitude, but also for the width of the polarization peak and the width and depth of the corresponding Stokes I profile, as well as the CLV of the continuum polarization. These five CLV curves provide powerful joint constraints on any future models for this line and its Hanle depolarization as a measure of the turbulent magnetic field.

The comparison between the different data sets shows that it is possible to obtain consistency after very careful corrections for the effects of spectral broadening and stray light have been made. It also highlights the great sensitivity of the results to these

corrections. The spread of the data points illustrates the degree of reproducibility of the results, but we have also shown evidence that at least some of this spread must be intrinsically solar. Thus a conspicuous kink in the CLV curve for the June 1994 data is most likely due to spatially varying Hanle depolarization on the Sun.

Such local fluctuations of the Hanle depolarization across the solar surface may be quantitatively interpreted in an almost model independent way if we observe the polarization in combinations of spectral lines with different sensitivities to the Hanle effect. We have started an observing program with ZIMPOL to calibrate and later exploit such line combinations as diagnostic tools for solar magnetoturbulence. A corresponding complementary program has also been started at IRSOL in the UV portion of the solar spectrum.

To better understand the scattering physics on the Sun and to exploit it for various diagnostic purposes we need to systematically observe the CLV behavior of many more lines in a similar, rather complete way as we have done for the Sr I line. The CLV of the scattering polarization is a sensitive function of the height variations of temperature and density in the upper photosphere, temperature minimum, and chromosphere, and it thus provides novel constraints for atmospheric modelling.

To gain more control of the Hanle and other magnetic-field effects we need to record the full Stokes vector rather than as here be limited to the Stokes Q and U parameters. Thus spectral signatures in Stokes U may reveal the possible presence of Hanle rotation of the plane of polarization and/or the transverse Zeeman effect, while signatures in Stokes V reveal longitudinal magnetic fields. The regime in which the Hanle and Zeeman effects mix is particularly interesting to explore. For such sensitive vector polarimetry we need improved control and/or compensation of the instrumental polarization. These various problems are different aspects of our long-term program to explore and make diagnostic use of the scattering polarization on the Sun.

References

Allen, C.W., 1973, Astrophysical Quantities, Third Edition. The Athlone Press, Univ. London

Auer, L.H., Rees, D.E., Stenflo, J.O., 1980, A&A 88, 302

Chandrasekhar, S., 1950, Radiative Transfer. Clarendon Press, Oxford

Donati J.-F., Semel M., Rees D.E., Taylor K., Robinson R.D., 1990, A&A 232, L1

Faurobert-Scholl, M., 1993, A&A 268, 765

Faurobert-Scholl, M., Feautrier, N., Machefert, F., Petrovay, K., Spielfiedel, A., 1995, A&A 298, 289

Keller, C.U., 1996, Solar Phys. 164, 243

Keller, C.U., Aebersold, F., Egger, U., Povel, H.P., Steiner, P., Stenflo, J.O., 1992, LEST Foundation Technical Report No. 53, Univ. Oslo

Leroy, J.L., 1977, In: Stenflo, J.O. (ed.), Measurements and Interpreta-
    tion of Polarization Arising in the Solar Chromosphere and Corona.
    Rep. Lund Observatory No. 12, p. 161
Mickey, D.L., Orrall, F.Q., 1974, A&A 31, 179
Povel, H.P., 1995, Optical Engineering 34, 1870
Povel, H.P., Keller, C.U., Stenflo, J.O., 1991. In: November L.J.
    (ed.), Solar Polarimetry. NSO/SP Summer Workshop Ser. No. 11,
    Sunspot, NM, p. 102
Semel, M., Donati, J.-F., Rees, D.E., 1993, A&A 278, 231
Stenflo, J.O., 1982, Solar Phys. 80, 209
Stenflo, J.O., 1994, Solar Magnetic Fields — Polarized Radiation Di-
    agnostics. Kluwer, Dordrecht

Stenflo, J.O., Keller, C.U., 1996, Nature 382, 588
Stenflo, J.O., Keller, C.U., 1997, A&A, in print
Stenflo, J.O., Baur, T.G., Elmore, D.F., 1980, A&A 84, 60
Stenflo, J.O., Twerenbold, D., Harvey, J.W., 1983a, A&AS 52, 161
Stenflo, J.O., Twerenbold, D., Harvey, J.W., Brault, J.W., 1983b, A&AS
    54, 505
Wiehr, E., 1975, A&A 38, 303